Journal of Renewable Materials

Tech Science Press

DOI: 10.32604/jrm.2021.013669

ARTICLE

Tensile Behavior of Strain Hardening Cementitious Composites (SHCC) Containing Reactive Recycled Powder from Various C&D Waste

Ruixue Wu[1], Tiejun Zhao[1], Peng Zhang[1], Dingyi Yang[2], Miao Liu[2] and Zhiming Ma[2,*]

[1]College of Civil Engineering, Qingdao University of Technology, Qingdao, 266033, China

[2]College of Civil Science and Engineering, Yangzhou University, Yangzhou, 225127, China

[*]Corresponding Author: Zhiming Ma. Email: 006879@yzu.edu.cn

Received: 16 August 2020 Accepted: 28 October 2020

ABSTRACT

This work investigates the feasibility of utilizing reactive recycled powder (RP) from construction and demolition (C&D) waste as supplementary cementitious material (SCM) to achieve a ductile strain hardening cementitious composites (SHCC). The recycled mortar powder (RMP) from mortar waste, recycled concrete powder (RCP) from concrete waste and recycled brick powder (RBP) from clay brick waste were first prepared, and the micro-properties and tensile behavior of SHCC containing various types and replacement ratios of RPs were determined. The incorporated RP promotes pozzolanic and filler effects, while the hydration products in cementitious materials decrease with RP incorporation; therefore, the incorporated RP decreases the compressive strength of SHCC. Attributed to the reduction in the matrix strength, the incorporated RP increases the crack-bridging extent and ductility of SHCC; the irregular micro-structure and high reactivity of RP also help the strain-hardening performance of the prepared SHCC. In addition, the strain-hardening performance of SHCC containing RMP and RBP is surperior to that of SHCC with RCP and is slightly lower than that of SHCC with fly ash (FA); for instance, the ultimate strain of SHCC containing 54% FA, RMP, RCP and RBP is 3.67%, 3.61%, 2.52% and 3.53%, respectively. In addition, the strain-hardening behavior of an SHCC doubled mix with FA and RMP or RBP has a similar ultimate strain and a higher ultimate stress than SHCC containing only FA.

KEYWORDS

Construction and demolition waste; recycled powder; strain hardening cementitious composites; tensile behavior

1 Introduction

Rapid urbanization construction dramatically increases the construction and demolition (C&D) waste worldwide [1,2]; for instance, the United States and China generate approximately 700 and 1800 million tons of C&D waste every year, respectively [3,4]. C&D waste is mainly disposed of by way of dumping and landfills, thereby taking up much land [5]; in addition, the inappropriate disposal of C&D waste causes some environmental pollution because of some hazardous components and extractable metal contained in C&D waste, which is not eco-friendly [2,6]. Therefore, some reclaiming technologies of C&D waste are developed, and most C&D wastes are currently recycled into recycled aggregate and

utilized in concrete preparation [7]. The properties of recycled aggregate are generally inferior to those of natural aggregate because recycled aggregate contains 30%–40% vol. old mortars [8]; thus, the employed recycled aggregate is generally detrimental to the mechanical properties and durability performance of concrete [9–12]. Some modification methods are developed to improve the properties of recycled aggregate concrete, such as the optimization of the preparation method [13], pre-soaking treatment [14], CO_2-curing treatment [15] and nano-material modification [16]; however, most of the modification methods and improvement technology are high cost, which is uneconomic [17].

Recently, some scholars have attempted to prepare recycled powder (RP) with a maximum size of 150 μm from C&D waste, and various RPs have been utilized as supplementary cementitious material (SCM) in preparing cement and concrete products [18−20]. The C&D waste mainly consists of mortar, concrete and brick wastes; thus, the mortar waste is recycled into recycled mortar powder (RMP), the concrete waste is ground into recycled concrete powder (RCP) and the brick waste is recycled into recycled brick powder (RBP). Decreasing the particle size of RP increases its reactivity, and the incorporated high fineness RP refines the pores of prepared cement-based material [21,22]; in addition, the utilized RP with a particle size above 75 μm is adverse to the micro-performance of cement-based material [23]. Previous studies further stated that incorporating an appropriate content and particle size of RP has less impact on the mechanical characterization of concrete, and an improvement in the compressive strength is reported for concrete with RP having a small particle size [24,25]; however, incorporating a high volume of RP (above 30%) is detrimental to the mechanical properties [26]. Furthermore, the utilized reactivity of the RP improves the permeability resistance; for example, when the median diameter of RBP was 8.5 μm, the chloride diffusion coefficients of concrete with 10% and 20% RP were 31.7% and 48.15% lower, respectively, than that of plain concrete [27]; when the median diameter of RP is 12.5 μm, Ma et al. [28] further stated that the capillary absorption coefficient of concrete with 30% RP was 13.2% lower than that of plain concrete. Therefore, the use of RP as SCM in concrete is feasible, which provides an eco-friendly and high-efficiency approach to reclaiming C&D waste.

Concrete has a high brittleness and low ductility, which limits the wide use of concrete material in construction applications under certain conditions. Therefore, the fiber-reinforced cementitious composites are developed to achieve a high ductility [29,30]. Especially for the strain hardening cementitious composites (SHCC), an excellent strain-hardening characteristic generates a high ultimate strain because of the crack-bridging action between the matrix and fiber [31]. However, traditional and common SHCC contains high contents of cement and fly ash (FA). The production of cement requires high energy consumption, and there is a large-scale lack of FA in current construction engineering; therefore, some investigations have been conducted to investigate the feasibility of utilizing RP from C&D waste for SHCC preparation [32,33]. Although previous investigations shows that fiber-reinforced cementitious composites with RP have good mechanical properties, the influence of the RP types and contents on the tensile behavior of SHCC has received little considerations.

Therefore, the overall goal of this study is to investigate the effects of RP types and replacement ratios on the micro-properties and tensile behavior of prepared SHCC. Based on the actual composition of C&D wastes, three types of RPs were used in this study, mainly including the RMP from mortar waste, the RCP from concrete waste and the RBP from brick waste; a common mix proportion of SHCC is defined as the control group, and the effects of the RP content on the micro-properties and tensile behavior are further investigated. Furthermore, this paper proposed a feasible approach to improving the strain-hardening performance of RP-prepared SHCC. RP derived from C&D waste is eco-friendly, and the findings in this study may promote an extensive utilization of RP in fiber-reinforced cementitious composites.

2 Materials and Experiments

2.1 RP Preparation and Fundamental Characteristics

Fig. 1 displays an approach to utilizing C&D waste to prepare RP. The C&D waste mainly consists of mortar, concrete and brick wastes, and thus, these wastes are ground into RMP, RCP and RBP, respectively. The water to cement ratios of the original mortar and concrete used in preparing RMP and RCP are both 0.5, as described in Tab. 1, and the initial strength of the original mortar and concrete is approximately 40.5 MPa and 37.6 MPa, respectively. The mortar, concrete and brick wastes were first crushed into aggregate with a maximum size of 10 mm; then, the aggregate was ground into coarse RP with a maximum size of 150 μm. Afterwards, these coarse RPs were further ground into an ultra-fine reactive RP by a planetary mill, and these ultra-fine reactive RPs were employed in SHCC preparation. Finally, the micro-performance and mechanical characterization were determined, and the tensile behavior of the SHCC containing various types and contents of RPs was the main focus.

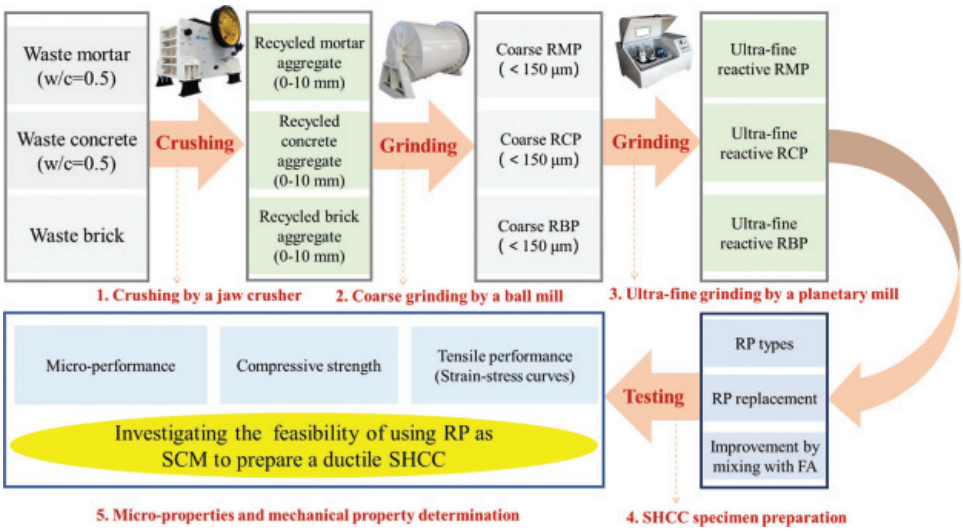

Figure 1: Process flow of RP preparation from C&D waste

Table 1: Mix proportion of original mortar and concrete used in preparing RP (kg/m^3)

Sample	w/b	Cement	Water	Sand	Natural coarse aggregate
Original mortar	0.5	450	225	1350	0
Original concrete	0.5	360	180	650	1190

Fig. 2a shows a comparison on the appearance of cement, FA, RMP, RCP and RBP. The appearance of RMP and RCP is similar to that of cement or FA; however, a red color was observed from RBP, because the original clay brick contains a high content of iron element. Generally, the particle size of RP is suggested to be below the particle size of cement when utilizing RP as SCM to replace cement in concrete; in this case, the filler effect of RP is promoted [22,34]. The particle size of cement, FA, RMP, RCP and RBP is determined by a laser particle sizer, and the results are shown in Fig. 2b. The median diameters of cement and FA are both approximately 18.0 μm, and the particle sizes of RMP, RCP and RBP are all approximately 10.0 μm. The utilized RMP, RCP and RBP have similar particle sizes, and in this case, the effects of the RP types and contents on the properties of prepared SHCC can be well characterized.

2.2 Mix Proportions and Specimens

Tab. 2 shows the mix proportion that is developed according to related literature [35–37]. On the one hand, the influence of the RP content on the tensile behavior of SHCC is considered in the mix design; the sample C-0RP stand for the control group without RP incorporation, and C-18RMP, C-36RMP and C-54RMP represent samples having 18%, 36% and 54% of cement replaced by the same weight of RMP. On the other hand, the influence of RP types on the tensile behavior of SHCC is also investigated, and C-54RMP, C-54RCP and C-54RBP represent samples in which the replacement ratios of RMP, RCP and RBP in the SHCC are all 54%. This work further gives a comparison of the tensile behavior of SHCC with the same contents of FA and various RPs (54% replacement ratios); in this case, the sample C-54FA is the control group that has been deeply investigated by many previous studies [38]. The SHCC sample that is mixed with both FA and RP is prepared to investigate the feasibility of improving the tensile behavior of RP-prepared SHCC; C-54(RMP+FA) sample is an SHCC containing 54% of the RMP and FA mixture (36% RMP and 18% FA).

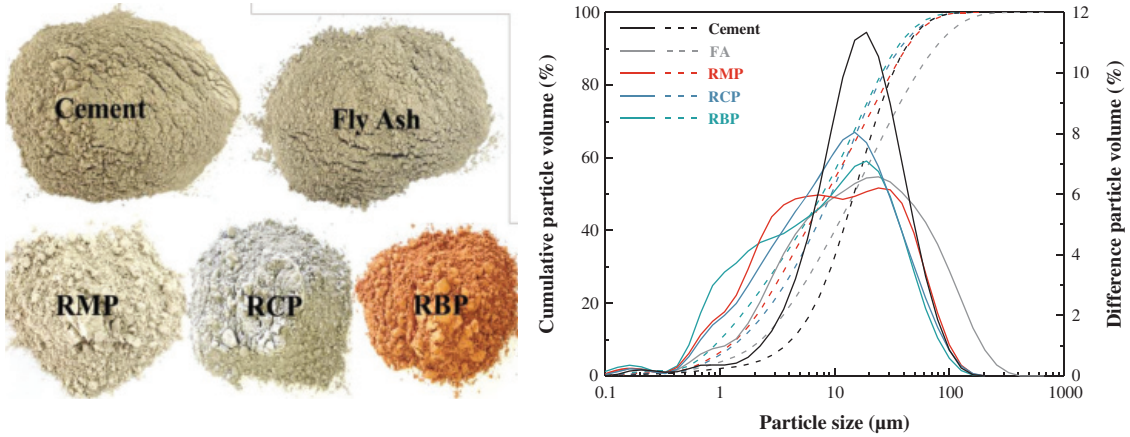

(a) (b)

Figure 2: Appearance and particle size of various types of RPs. (a) Appearance. (b) Particle size distribution

The SHCC samples were first prepared according to the mix proportion shown in Tab. 2. Because RP with an irregular micro-structure absorbs more water than the cement, the incorporated RP results in an increase in the water reducer amount in the SHCC when all the mixtures have a similar fluidity. The water demand ratio of RP was determined according to Chinese standard GB/T1596-2017, and the water demand ratio of cement, RMP, RCP and RBP was 1.00, 1.09, 1.10, 1.07, respectively, when the particle size of various RPs is approximately 10 μm. In addition, the suggested flow expansibility of SHCC should be (185 ± 5) mm according to Chinese standard GB/T 15234-2016; therefore, the flow expansibility of mix proportion with various types and contents of RP was kept at (185 ± 5) mm by adjusting the amount of water reducer. The incorporation of RP increases the water demand of mixture, and more water reducer is required in the SHCC prepared with RP incorporation, as shown in Tab. 2. In particular, RCP has a higher requirement than RMP and RBP for the amount of water reducer. The binders of cement, RP and FA were first mixed at low-speed for 2 mins by a machine mixer, and then, the water, PVA fiber and water reducer were mixed with the binders at high-speed for 3 mins; finally, the obtained mixtures were placed in steel moulds to prepare the SHCC samples, and three samples were prepared for each mix proportion of SHCC. These samples after hardening were cured for 28 d (relative humidity ≥ 95% and temperature at 20 ± 2°C). As shown in Fig. 3, the appearance of RMP- and RCP-prepared SHCC is similar to that of the control group. However, because the color of RBP is red, the appearance of RBP-prepared SHCC is different from the appearance of the control group.

Table 2: Mix proportion of SHCC with RP (kg/m^3)

Specimen	Cement	Recycled powder (RP)	Fly ash (FA)	Water content	Sand	PVA fiber (12 mm)	Water reducer
C-0RP (Control group)	1200	0	0	395	550	26	3
C-54FA (Control group)	550	0	650	395	550	26	1
C-18RMP	982	218 (RMP)	0	395	550	26	3.5
C-36RMP	768	432 (RMP)	0	395	550	26	4
C-54RMP	550	650 (RMP)	0	395	550	26	4.5
C-18RCP	982	218 (RCP)	0	395	550	26	3.6
C-36RCP	768	432 (RCP)	0	395	550	26	4.2
C-54RCP	550	650 (RCP)	0	395	550	26	4.8
C-18RBP	982	218 (RBP)	0	395	550	26	3.4
C-36RBP	768	432 (RBP)	0	395	550	26	3.8
C-54RBP	550	650 (RBP)	0	395	550	26	4.2
C-54(RMP+FA)	550	432 (RMP)	218	395	550	26	2.5
C-54(RCP+FA)	550	432 (RCP)	218	395	550	26	2.6
C-54(RBP+FA)	550	432 (RBP)	218	395	550	26	2.3

2.3 Compressive and Tensile Strength Determination

The compressive and tensile strengths were determined to evaluate the mechanical properties of the RP-prepared SHCC. The cube sample with a size of 70.7 mm is utilized in a compressive strength test according to "Standard for test method of performance on building mortar" (Chinese standard JCJ/T70-2009). A dogbone-shaped sample is utilized in the tensile test; the sample size is designed according to "Recommendations for design and construction of high performance fiber reinforced cement composites with multiple fine cracks (HPFRCC)" that is recommended by the Japan Society of Civil Engineers (JSCE), and the size of the SHCC sample is described in Fig. 3a. Fig. 3b shows an image of the tensile test used to determine the tensile behavior of the RP-prepared SHCC. The applied loads are provided by a universal mechanical testing machine, and the rate of the applied load is 0.1 mm/min. The load applied on the SHCC can be determined by the employed mechanical testing machine, and meanwhile, the displacement of a determined length (80 mm) is collected by testing device; therefore, the stress and strain of the SHCC can be further calculated from the obtained data of the applied load and displacement.

In addition, the crack development of SHCC with various types and contents of RPs is also observed to evaluate the strain-hardening performance. The micro-characteristics correspond to the macro-performances of cement-based materials [39–41]. To better understand the influence of RP incorporation on the tensile strength of SHCC, the micro-properties of cement composites with various types and contents of RPs are further determined. The micro-structure of RP is determined by scanning electron microscopy (SEM) determination, and the composition of RP and the prepared cement-based material is further measured by X-ray diffraction (XRD). In addition, Fourier transform infrared spectroscopy (FTIR) is conducted to reveal the hydration products of SHCC containing various RPs.

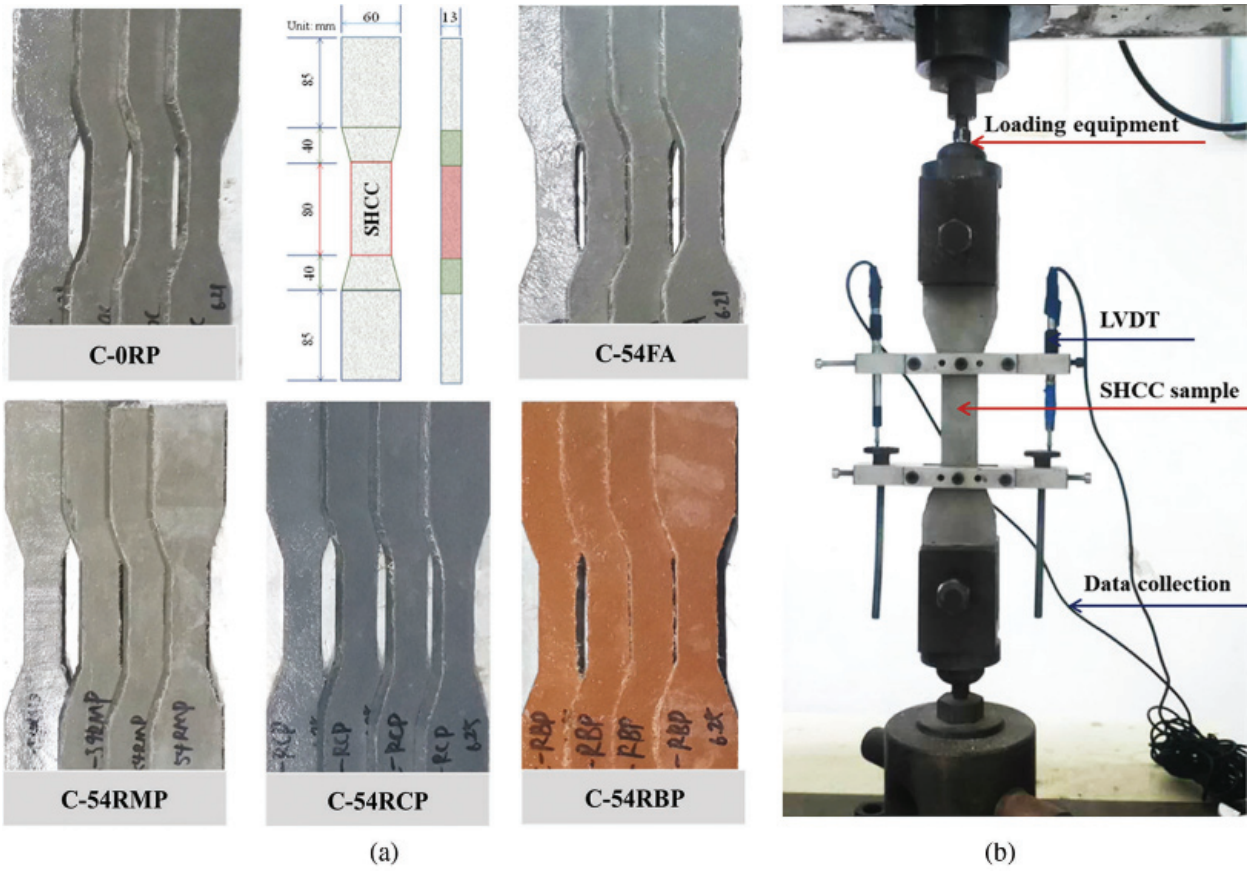

Figure 3: Specimens and tensile strength test. (a) Specimens used in the tensile test and (b) Uniaxial tensile test

3 Results and Discussion

3.1 Micro-Characteristics and Activity Index of RP

Fig. 4 SEM images of micro-structure of cement, FA and various RPs. For various binders with the same measuring scale, the particle size of RP is lower than that of cement and FA. Especially for the micro-structure of FA, a spheroidal structure is observed, which helps the micro-sphere effect and improves the workability of the cement-based material. However, it can be seen that the micro-structures of RMP, RCP and RBP are all irregular, and more edges and corners can be observed; in addition, some hydrated cementitious products are observed from the micro-structure of RMP and RCP. The irregular micro-structure and high specific surface area of RP results in a decrease in the workability of the mixture [26,42].

Fig. 5a shows the XRF results of cement, FA and various RPs. RMP contains high content of silicon dioxide that is derived from sand, and the calcium oxide is mainly from the hydration products and unhydrated cement particles in the original mortar waste. RCP contains high content of calcium oxide and silicon dioxide, and the calcium oxide mainly comes from the hydration products and natural coarse aggregate in the original concrete waste; in addition, these calcium compounds are less reactive than the silicon dioxide and aluminium oxide that takes part in the pozzolanic reaction. RBP prepared from sintered clay brick mainly consists of silicon dioxide and aluminium oxide, and these components help the pozzolanic reaction and improve the reactivity of RBP. A similar conclusion can be drawn from XRD results of various binders, as shown in Fig. 5b; in particular, the RMP contains some calcium hydroxide that is from the unhydrated cement particles in the original mortar waste, and a high content of calcium carbonate exists in RCP.

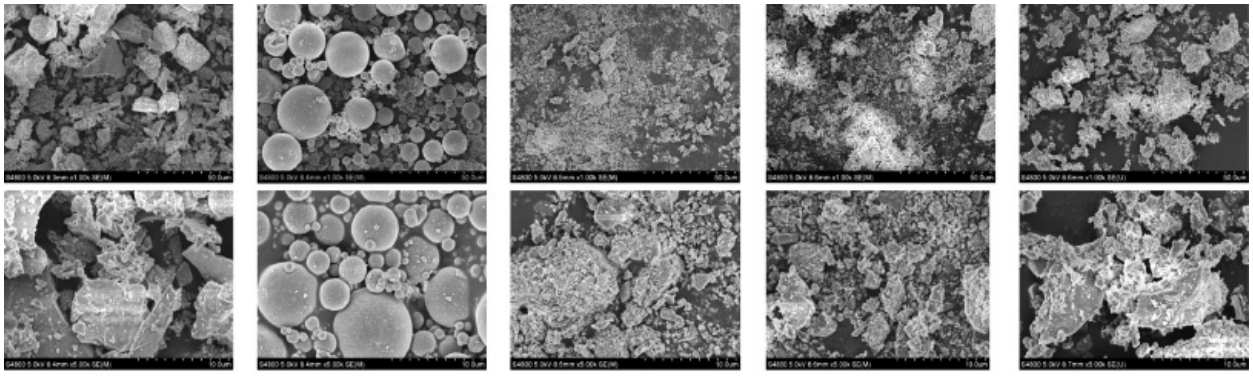

Figure 4: Micro-structure of cement, FA and various RPs (50 μm and 10 μm). (a) Cement. (b) FA. (c) RMP. (d) RCP. (e) RBP

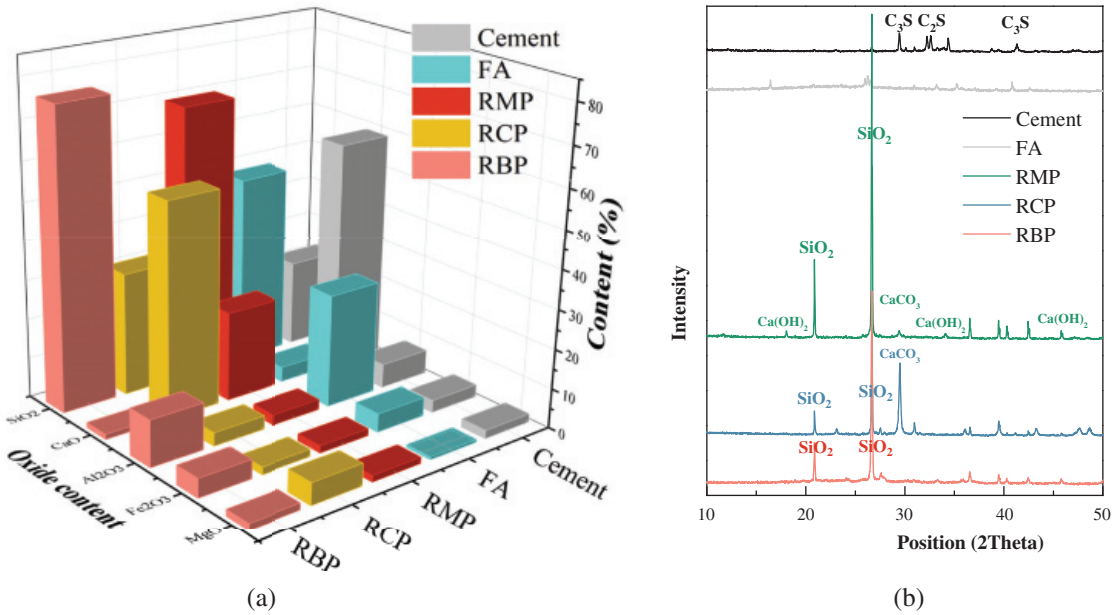

Figure 5: Composition of cement, FA and various RPs. (a) XRF. (b) XRD

The activity index of FA and RP was determined according to the British standard BS EN-450 and Chinese standard GB/T-1596. The cement mortar with a water to binder ratio of 0.50 was used to determine the activity index of RP; the mix proportion of plain mortar consists of cement (450 g), water (225 g) and fine sand (1350 g), and the mix proportion of RP-prepared mortar consists of cement (315 g), RP (135 g), water (225 g) and fine sand (1350 g) [34]. The samples after hardening were placed in a curing room for 28 d, the compressive strength of the plain mortar and RP-prepared mortar was determined, and the ratios of the RP mortar strength to the plain mortar strength is defined as the activity index of RP, as shown in Fig. 6. The Chinese standard GB/T-1596 states that the activity index of SCM should be above 70%. The determined activity indexes of various RPs are all above 70%, which means that RP can to be utilized as an SCM, and the high activity index of RP is helpful to the properties of prepared cementitious composites. Due to the high content of silicon dioxide or aluminium oxide in high fineness RBP and RMP, the reactivity of RBP and RMP used in this work is higher than that of FA; for

instance, the 3 d activity indexes of FA, RMP and RBP are 70.8%, 73.2% and 73.6%, respectively, and the 28 d activity indexes of FA, RMP and RBP are 83.2%, 85.5% and 87.0%, respectively. The RCP contains some inert components and hydrated substances, thereby decreasing the reactivity of RCP; however, the high fineness RCP still has a relatively high reactivity (the 28 d activity index is 78.7%) because of its filler effect and can be utilized as an SCM in SHCC preparation.

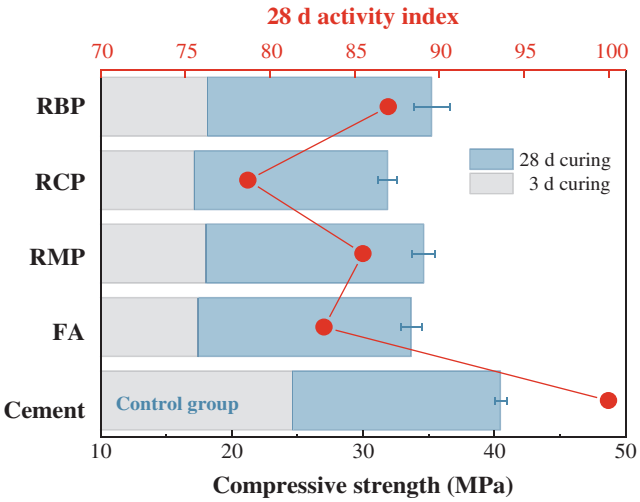

Figure 6: Activity index of FA and various RPs

3.2 Micro-Properties of Cementitious Composites with Various RPs

Fig. 7 shows the FTIR results of cement paste containing various types and contents of RPs. The peak at approximately 970 cm^{-1} is attributed to the Si-O stretching vibration and the formation of the C-S-H gel [43]. The peak value of the Si-O stretching vibration increases with RP incorporation, which means that $H_2SiO_4^{2-}$ happens to form silicon-oxygen tetrahedra with a high polymerization degree; in this case, incorporating RP promotes the hydration degree of cement-based material and improves the polymerization degree of C-S-H. In addition, the peak value of the Si-O stretching vibration of cement paste with RBP is higher than that of cement paste with RMP and RCP, which indicates that the cement paste with RBP has the most Si-O stretching vibrations and the highest polymerization degree of C-S-H. The peak approximately 1421 cm^{-1} is attributed to the C-O stretching vibration and the formation of $CaCO_3$ [43]; the results show that the used RCP significantly increases the peak value of the Ca-O stretching vibration, because the original concrete used to prepare RCP contains natural coarse aggregates that mainly consist of $CaCO_3$; in addition, RMP incorporation slightly increases the content of $CaCO_3$ that is mainly derived from the cement paste in the original mortar waste.

Fig. 8 shows the XRD results of the paste with various types and contents of RPs. For the cement paste with RMP (Fig. 8a), the incorporated RMP results in an increase in the content of silicon dioxide and calcium carbonate content; the silicon dioxide is mainly from natural sand, and the calcium carbonate is derived from the cementitious material in the original mortar. For cement paste with RCP, a significant increase in the calcium carbonate content is observed (Fig. 8b), and this calcium carbonate is mainly derived from the natural coarse aggregate in the original concrete. For cement paste containing RBP (Fig. 8c), the silicon dioxide concentration increases with RBP incorporation, while incorporated RBP decreases the concentration of calcium carbonate and calcium hydroxide in cement paste; the increased silicon dioxide content promotes the pozzolanic reaction, while the decreased calcium carbonate and calcium hydroxide contents represent a reduction in the amount of hydration products. Fig. 9 further shows the various

elemental contents of cement paste with and without RBP. Due to the high content of silicon in RBP, the utilized RP significantly increases the silicon content of the cement paste, while the calcium content decreases with RP incorporation. Such as, the calcium content is 203.0% higher than the silicon content in cement paste without RBP, while the calcium content is 54.5% lower than the silicon content in cement paste with 54% RBP. The significant decrease in the calcium content leads to an obvious decrease in the amount of hydration products in the cementitious composites. Moreover, the incorporated RBP also increases the iron and aluminium elemental contents of cement-based materials.

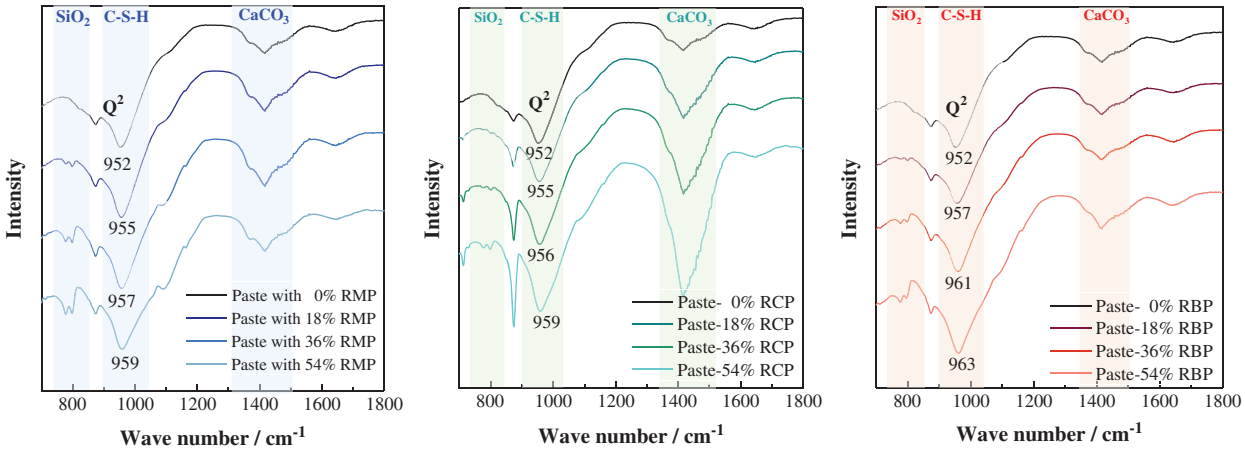

Figure 7: FTIR spectra of cement paste containing various types and contents of RP. (a) Cement paste with RMP. (b) Cement paste with RCP. (c) Cement paste with RBP

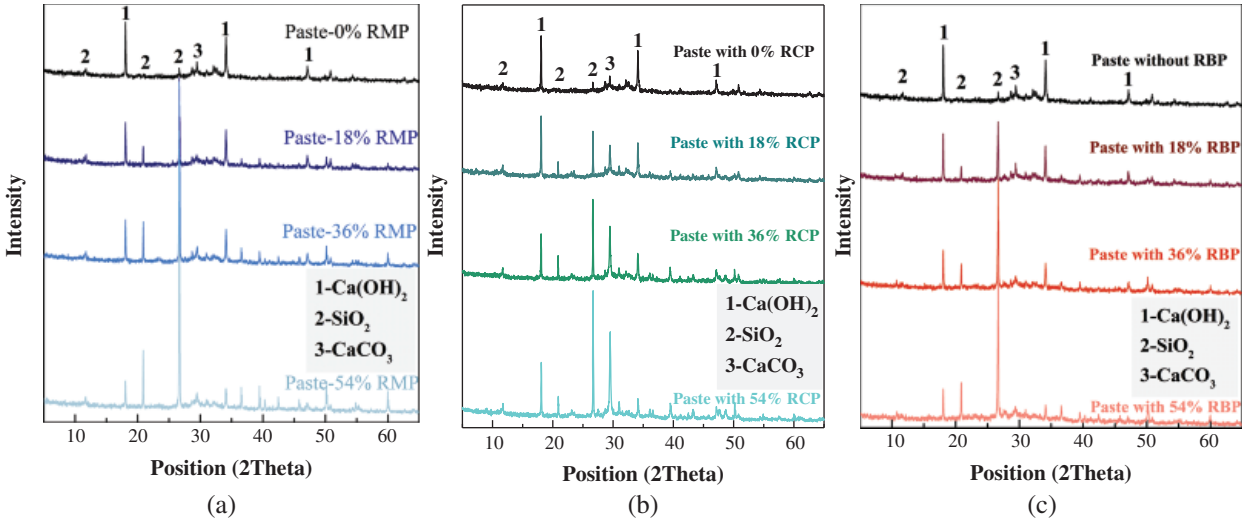

Figure 8: XRD results of cement paste with RP (28d). (a) Cement paste with RMP, (b) Cement paste with RCP and (c) Cement paste with RBP

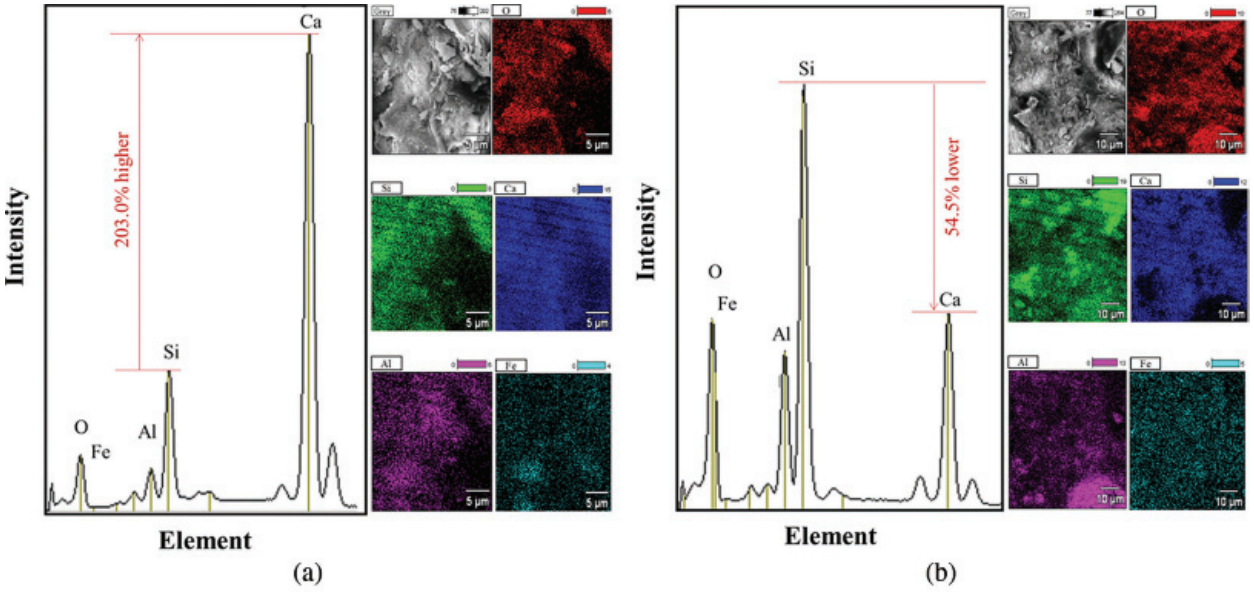

Figure 9: Elemental content of cement paste with and without RBP. (a) Paste without RBP and (b) Paste with 54% RBP

3.3 Compressive Strength of SHCC Containing RP

The 3 d and 28 d compressive strength of SHCC containing various types and replacement ratios of RPs were determined, and the results are shown in Figs. 10a–10c. The incorporated RP results in a decrease in the compressive strength, and the reduction in the compressive strength is significant when the RP content is above 36%. For instance, the compressive strength of SHCC containing 18%–54% RMP is 15.7%–44.3% lower than that of SHCC without RMP, and the results are 25.6%–48.3% for SHCC with 18%–54% RCP, and they are 11.7%–42.4% for SHCC with 18%–54% RBP. This is because RP incorporation decreases the amount of hydration products, thereby decreasing the compressive strength of the SHCC. In addition, the adverse impact of RP incorporation on the compressive strength decreases with increasing curing days, and this is because the increased curing duration promotes the filler and pozzolanic effects of the reactive RP; for instance, the 3 d compressive strength of SHCC containing 54% RMP, RCP and RBP are 49.4%, 56.8% and 47.2% lower than that of SHCC without RP, while the 28 d compressive strength of SHCC incorporating 54% RMP, RCP and RBP are 44.3%, 48.3% and 42.4%.

Comparing the results shown in Figs. 10a–10c, SHCC containing RMP and RBP have a higher compressive strength than SHCC containing RCP when the replacement ratios of various RPs are the same. For example, the compressive strength of SHCC containing 54% of RMP, RCP and RBP are respectively 40.7 MPa, 37.8 MPa and 42.2 MPa after 28-d curing. This is because the activity index of RMP and RBP is higher than that of RCP, as shown in Fig. 6. In addition, RMP and RBP have higher silicon oxide and aluminium oxide contents than RCP, and these active substances promote the pozzolanic reaction, which improves the properties of the prepared SHCC; however, RCP has a high calcium carbonate content, which hardly promotes the secondary hydration reaction of the cement-based material. Furthermore, Fig. 10d shows the compressive strength of SHCC with RP and FA, and incorporated FA decreases the compressive strength of SHCC when partially replacing RP with the same weight of FA. The compressive strength of SHCC with the FA and RP mixture is lower than that of SHCC with only RP; for instance, the 28 d compressive strength of SHCC with FA and RP mixture are 1.7%–8.1% lower than that of SHCC with only RP when total SCM content is 54%. This is mainly

because the particle size of RP is lower than that of FA, and thus, the filler effect of FA is lower than that of RP; this is especially true for RMP and RBP with a high content of silicon dioxide, and the activity index of RMP and RBP is higher than that of FA; therefore, the compressive strength decreases when replacing RP with FA in SHCC.

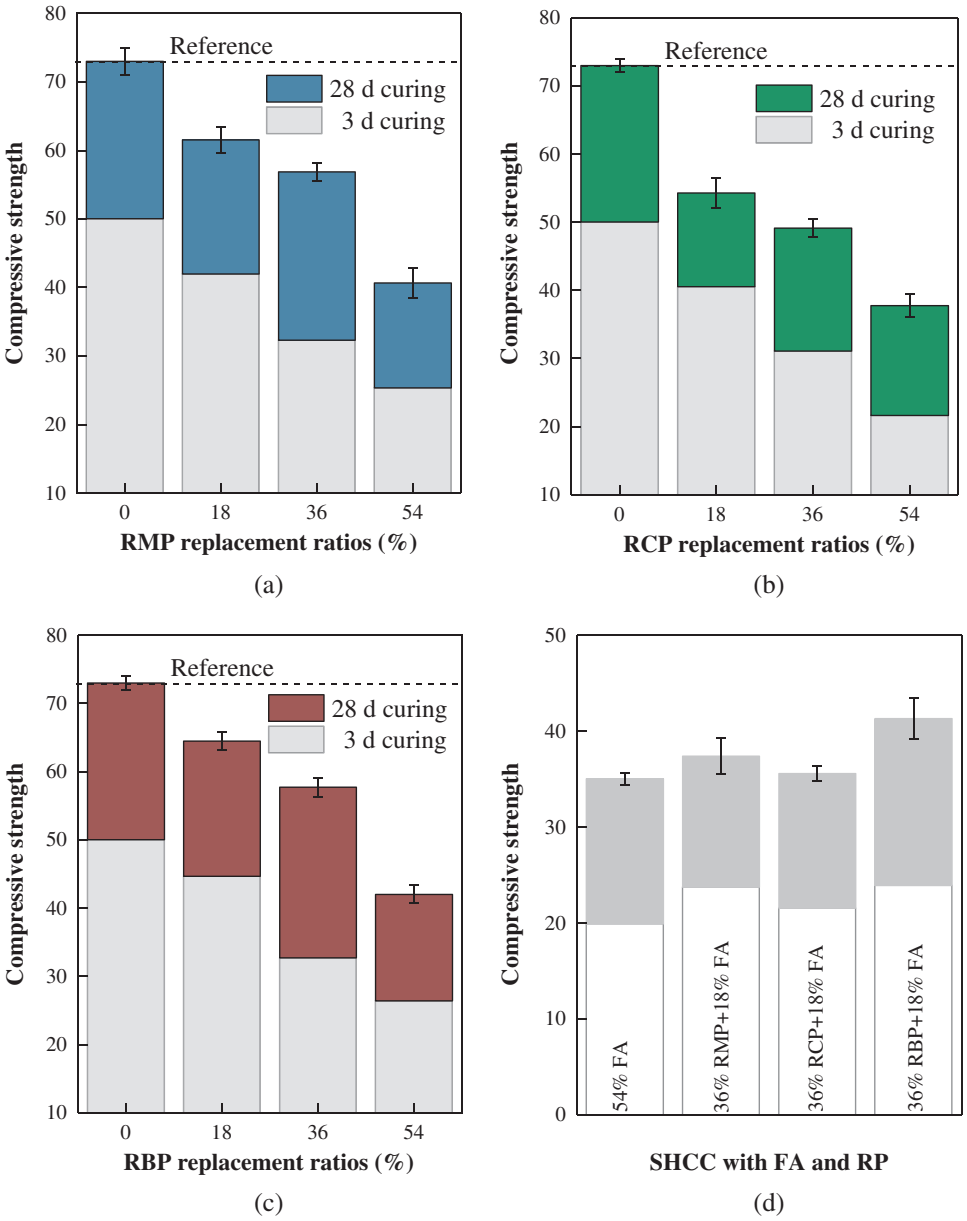

Figure 10: Compressive strength of SHCC containing RP. (a) SHCC with various RMP contents, (b) SHCC with various RCP contents, (c) SHCC with various RBP contents and (d) Double mixing with FA and RP

3.4 Tensile Behavior of SHCC with Reactive RP

This section investigated the influence of the RP types and contents on the tensile behavior of prepared SHCC. Fig. 11 shows the stress-strain curve of SHCC with various replacement ratios of RMP. The ultimate

strain of SHCC increases with RMP incorporation, and the increase is significant when the RMP replacement ratios are above 36%; for instance, the ultimate strain of C-18RMP, C-36RMP and C-54RMP are 15.9%, 117.0% and 310.2% higher than that of the control group. Meanwhile, the incorporated RMP decreases the ultimate stress of SHCC; for example, the ultimate stress of C-18RMP, C-36RMP and C-54RMP are 6.2%, 15.5% and 18.0% lower than that of the control group without RMP, respectively. In particular, the strain-hardening performance of the SHCC improves with increasing the RMP replacement ratios, RMP incorporation decreases the amplitude of the stress-strain curves, and multiple cracks form and develop with RMP incorporation; especially for SHCC containing 54% RMP, a good strain-hardening performance can be observed. Fig. 11 further shows the actual crack distribution of the SHCC containing various contents of RMP, and many cracks can be observed on the surface of SHCC with RMP incorporation. In addition, the incorporated RP tends to decrease the crack width of SHCC, and one previous study that the maximum crack width of cementitious material incorporating 25% and 50% RP is approximately 14.2% and 18.5% lower than that of reference cementitious material without RP [19].

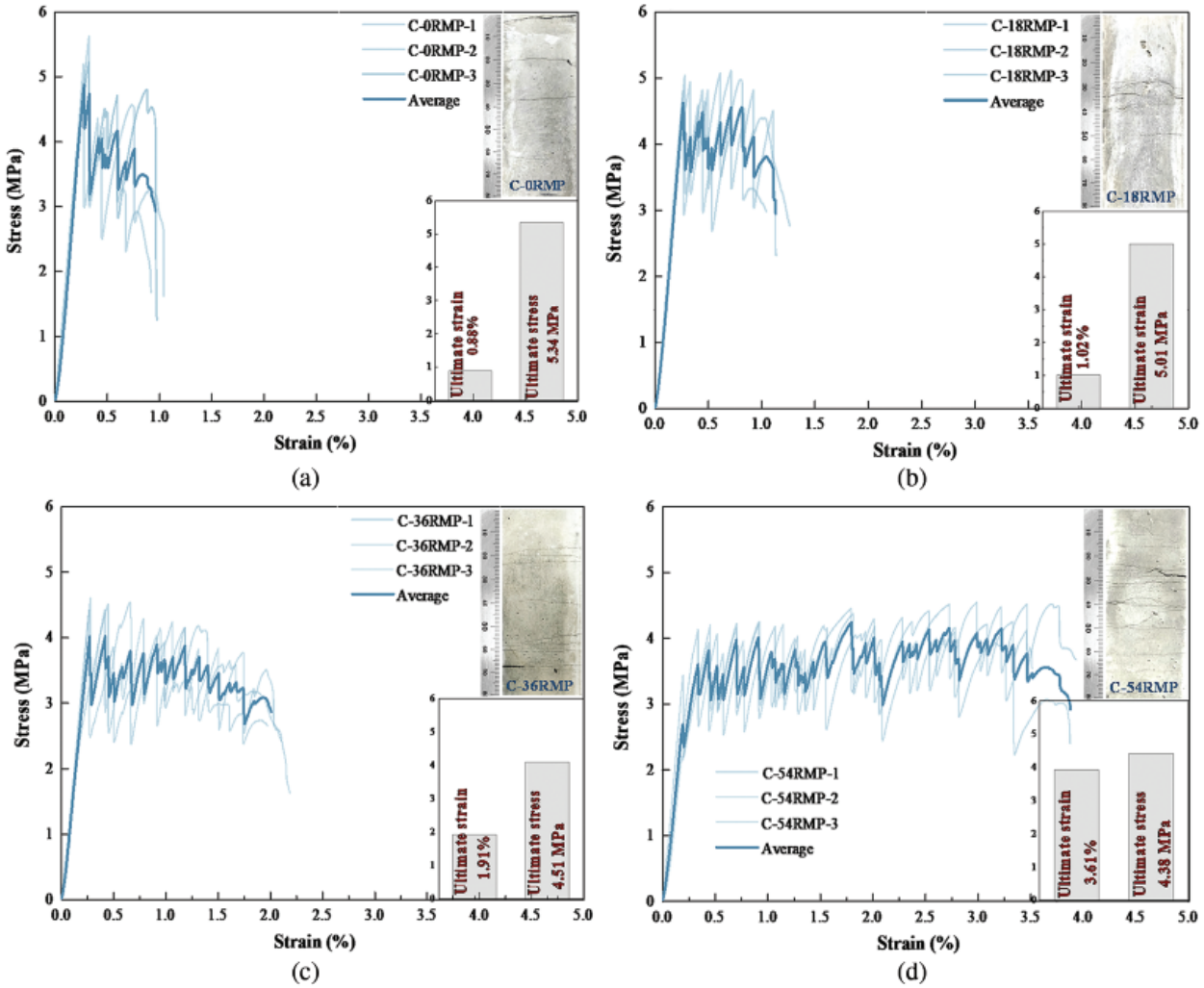

Figure 11: Stress-strain curves of RMP-prepared SHCC under uniaxial tensile load. (a) Without RMP (Control group), (b) Replacing cement with 18% RMP (C-18RMP) and (c) Replacing cement with 36% RMP (C-36RMP). (d) Replacing cement with 54% RMP (C-54RMP)

The above mentioned results indicate that the utilized RMP improves the strain-hardening performance of SHCC. The crack-bridging action in the SHCC without RMP is mainly caused by the interaction between the C-S-H gel in the cement paste and PVA fibers, and in this case, the crack-bridging action is weakening because of the brittle characteristics and high strength of the C-S-H gel; moreover, the high matrix strength is adverse to the strain-hardening performance of the SHCC. The incorporation of RMP decreases the matrix strength of SHCC, thereby improving the strain-hardening performance of SHCC; in addition, the high fineness and irregular micro-structure of RP also helps the frictional force between the paste and PVA fibers; a similar phenomenon is also reported by Yu et al. [44], who explained that the irregular particle morphology and rough surface of RP resulted in an increase in the connectivity between the paste and the fiber, and the frictional force that provided fiber pull-out increased with RP incorporation. Moreover, the low matrix strength and the superior interface properties between the fiber and the paste improve the strain-hardening and multiple cracking performances [45]; when replacing the cement with the same weight of RMP, the decreased strength of the cement-based material results in the cracking strength being below the maximum crack-bridging force, and in this case, the PVA fiber is prone to pull-out rather than fracture failure, thereby improving the strain-hardening performance.

However, the incorporated RMP decreases the ultimate stress of SHCC, because RMP incorporation decreases the total amount of hydration products in SHCC. Note that there is no significant decrease in the ultimate stress of SHCC when the RMP replacement ratios range from 36% to 54%. This is because the incorporated RMP improves the strain-hardening performance of SHCC, and in this case, the adverse effect of the reduction in the amount of hydration products and mechanical properties is declined. In addition, the w/b ratio of SHCC is 0.33, and some un-hydrated cement particles can further react with the RMP particle by a pozzolanic reaction and secondary hydration reaction; therefore, there is no significant decrease in the ultimate stress of SHCC with RMP incorporation up to 54%.

Fig. 12 shows the stress-strain curves of SHCC with various RCP replacement ratios. The ultimate strain increases and the ultimate stress decreases with increasing RCP contents; such as, the ultimate strain of C-18RCP, C-36RCP and C-54RCP is 32.9%, 97.7% and 186.4% higher than that of the control group without RMP, while the ultimate stress of C-18RCP, C-36RCP and C-54RCP is 10.1%, 19.1% and 21.3% lower than that of the control group. For SHCC without RCP, the main crack rapidly occurs and develops to failure with the increase of applied load; however, for SHCC containing 54% RCP, the more cracks forms and develops on the surface of SHCC, thereby increasing the strain-hardening performance and ultimate strain. This is because the incorporated RCP results in a decrease in the matrix strength and improves the strain-hardening performance of prepared SHCC.

Fig. 13 shows the stress-strain curves of SHCC with various RBP contents, and a similar conclusion is drawn. The incorporation of RBP increases the ultimate strain and decreases the ultimate stress of prepared SHCC; such as, the ultimate strain of SHCC with C-18RBP, C-36RBP and C-54RBP is 30.7%, 97.7% and 301.1% higher than that of the control group, and the ultimate stress of C-18RBP, C-36RBP and C-54RBP is 8.1%, 13.5% and 16.7% lower than that of the control group. In particular, the multiple cracks uniformly distribute on the surface of C-54RBP sample, and some tiny cracks on SHCC with 54% RBP are closed after unloading. This is because the strength of cement matrix decreases with RBP incorporation, thereby improving the strain-hardening behavior of SHCC; in addition, the high fineness and reactive RBP contains high SiO_2 content, and these amorphous compound promotes the pozzolanic reaction and filler effect, which also helps the mechanical properties [34].

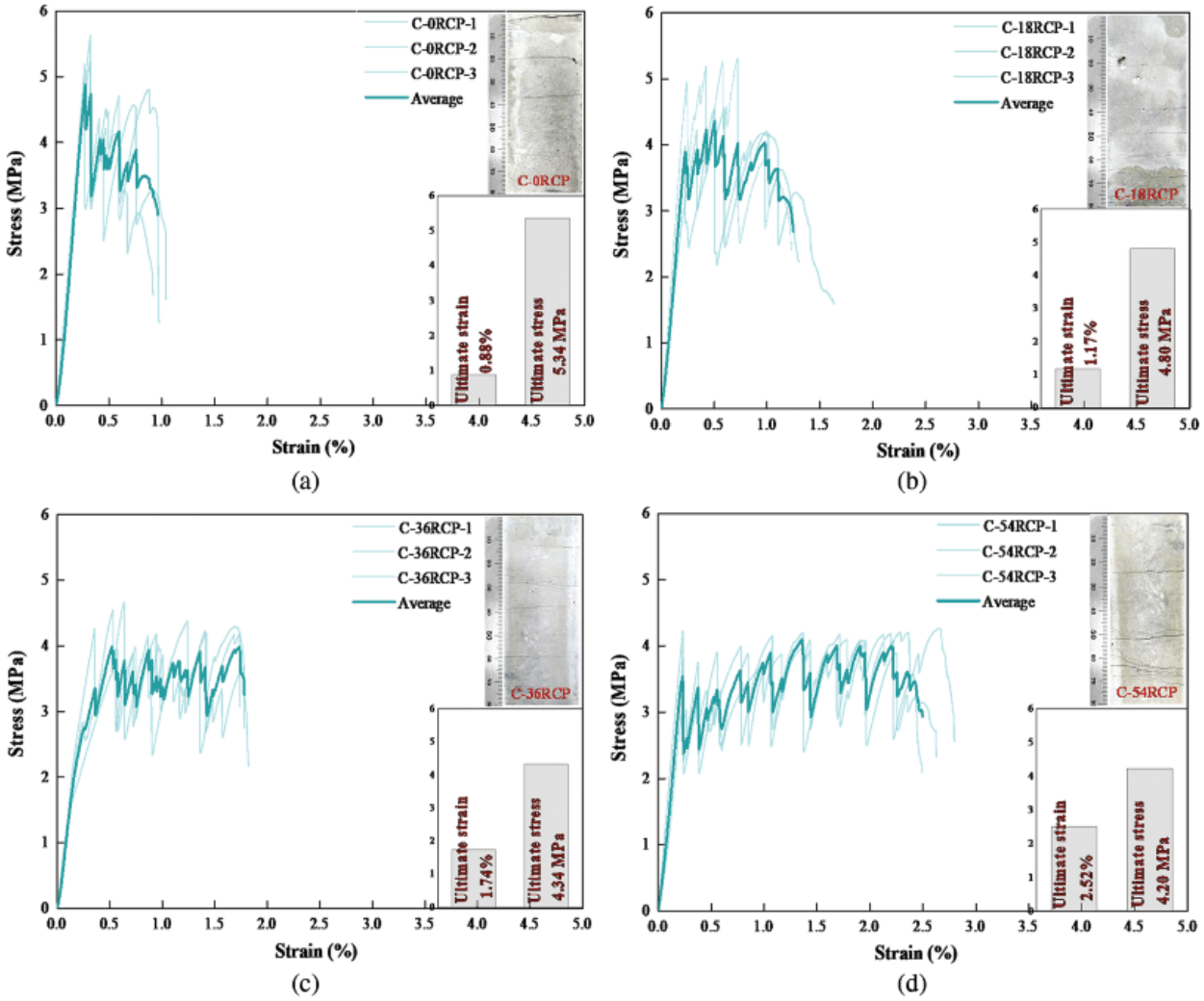

Figure 12: Stress-strain curves of RCP-prepared SHCC under an uniaxial tensile load. (a) Without RCP (Control group), (b) Replacing cement with 18% RCP (C-18RCP), (c) Replacing cement with 36% RCP (C-36RCP) and (d) Replacing cement with 54% RCP (C-54RCP)

Fig. 14 shows the tensile behavior parameters of SHCC with various types and replacement ratios of RPs. The utilized RP increases the ultimate strain and decreases the ultimate stress of SHCC. Moreover, the SHCC with RMP and RBP have a higher ultimate strain and stress than the SHCC with RCP when the replacement ratios of the various RPs are the same; this is because the activity index of RMP and RBP is higher than that of RCP, and the micro-structure and tensile behavior of the RMP- and RBP-prepared SHCC are better than those of RCP-prepared SHCC when the RP replacement ratios are the same. Fig. 15 shows a comparison of the strain-stress of SHCC with the same replacement ratios of FA and RP. As shown in Fig. 15a, the common SHCC with a 54% FA replacement ratio has an excellent strain-hardening performance, and the ultimate strain is approximately 4%; multiple cracks uniformly distribute on the surface of C-54FA, and the observed crack number at an 80 mm length in C-54FA after failure is 24-32N. Fig. 15b shows the stress-strain curves of SHCC containing 54% of RMP, RCP and RBP. The ultimate stress of C-54RMP and C-54RBP is slightly higher than that of C-54RCP, and the ultimate strain of C-54RMP and C-54RBP is higher than that of C-54RCP, which means that the SHCC

with RMP and RBP has a better strain-hardening performance than SHCC with RCP. Comparing the stress-strain curves of the SHCC with the same content of FA and RP, the ultimate stress of the RP-prepared SHCC is higher than that of the FA-prepared SHCC, while the ultimate strain of the RP-prepared SHCC is lower than that of the FA-prepared SHCC; the ultimate strain of C-54RMP and C-54RBP is slightly lower than that of C-54FA, while the ultimate strain of C-54RCP is much lower than that of C-54FA. Fig. 16 shows the SEM images of the interface between fiber and matrix in ECC/SHCC with and without RP [19]; the fiber surface was smooth with slight matrix particle adhesives in reference cementitious composites; while the lateral surface of fiber in cementitious composites incorporating 25% RP was stuck to more matrix articles during the pullout process leading to a higher tensile strength; and some fibers were grooved severely on the surface or even fractured during the pull-out process.

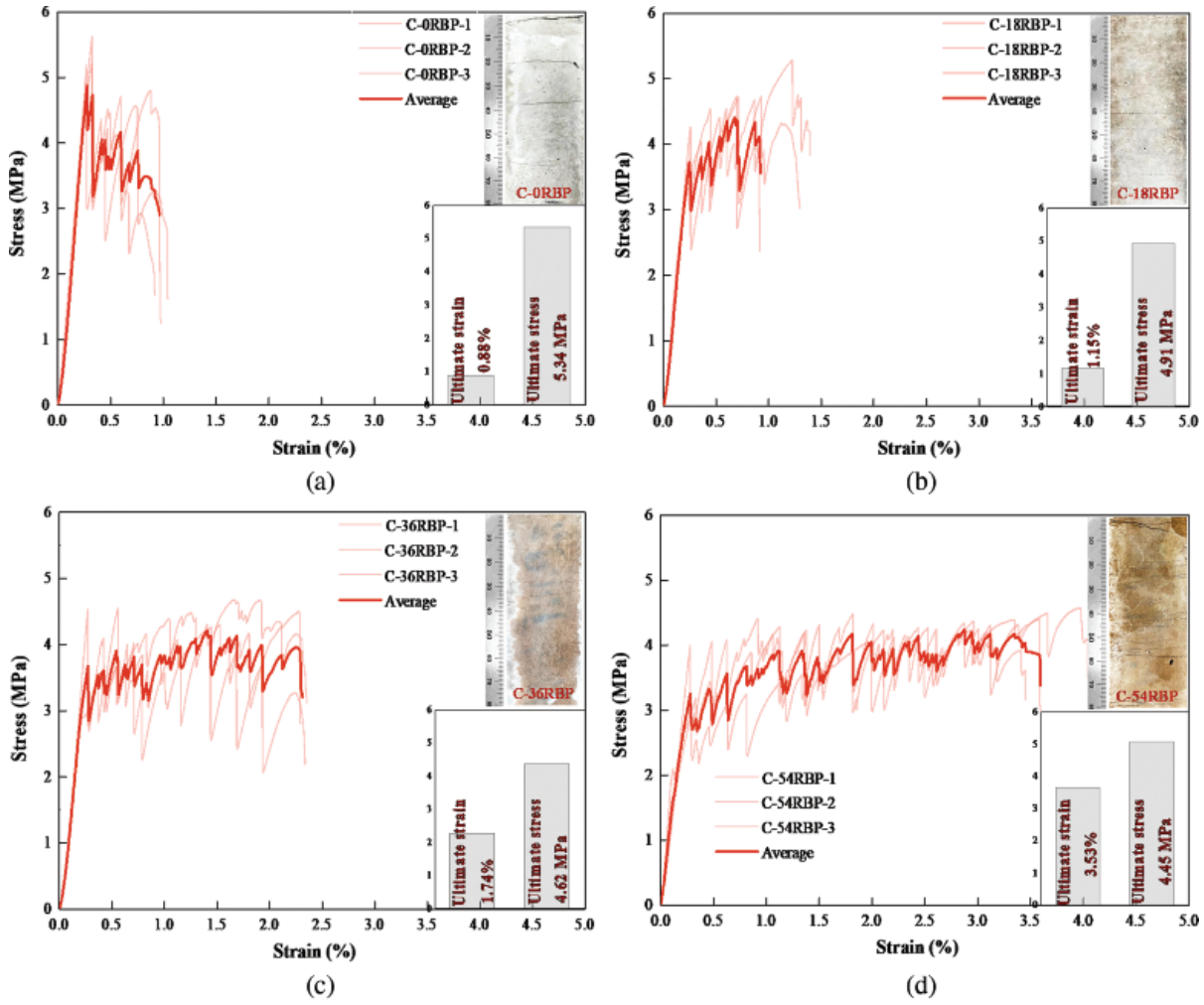

Figure 13: Stress-strain curves of RBP-prepared SHCC under an uniaxial tensile load. (a) Without RBP (Control group), (b) Replacing cement with 18% RBP (C-18RBP), (c) Replacing cement with 36% RBP (C-36RBP) and (d) Replacing cement with 54% RBP (C-54RBP)

For SHCC containing FA, the improvement in the strain-hardening performance is because FA contains a high content of non-ionizing calcium ions and dilutes the calcium ion concentration of the cement paste, thereby decreasing the bridging strength between the matrix and PVA fiber; PVA fiber is easy to pull-out from

the matrix rather than pull-cut, and in this case, the strain-hardening performance of the SHCC is improved with FA incorporation [46]. For SHCC containing RP, on the one hand, the RP incorporation decreases the matrix strength, thereby improving the ductility and strain-hardening performance of the SHCC; on the other hand, the utilized RP with a small particle size and irregular micro-structure results in a larger frictional force between the paste and PVA fiber than FA results in when incorporated in SHCC, and thus, the RP-prepared SHCC also has a good strain-hardening performance; for example, when 50% and 100% of FA in fiber-reinforced cementitious composites is replaced with the same weight of RP, Yu et al. [44], through a single-crack tension test, found that the frictional force between the matrix and fiber in cementitious composites with RP was 18%–40% higher than the frictional force in cementitious composites with FA. However, the improvement in the strain-hardening performance of SHCC with RMP and RBP is superior to that of SHCC with RCP, because the reactivity of RMP and RBP is higher than that of RCP, as shown in Fig. 6.

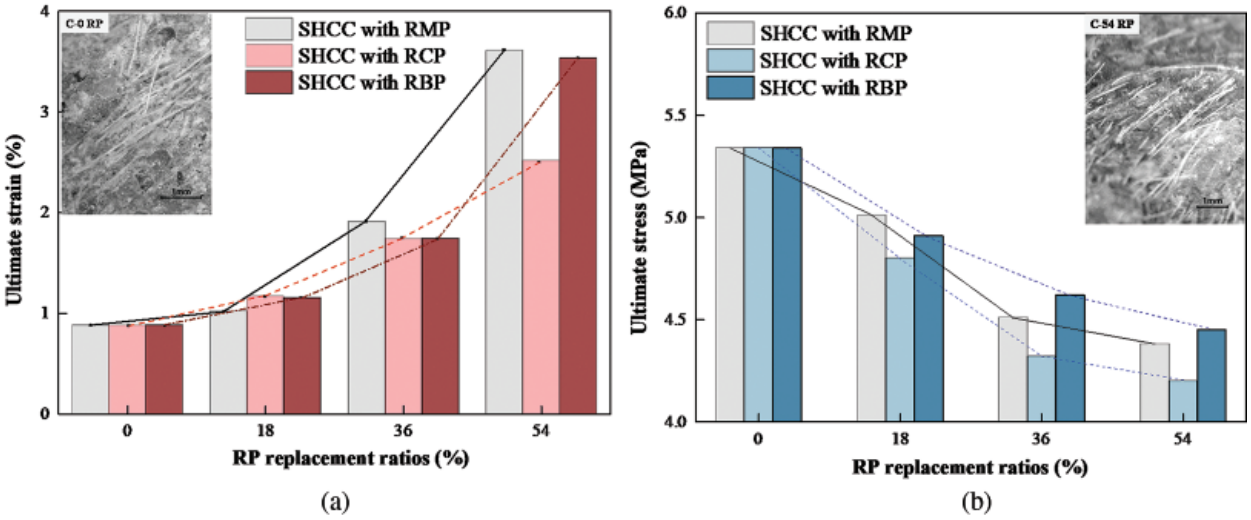

Figure 14: Ultimate strain and stress of SHCC containing various types and replacement ratios of RPs. (a) Ultimate strain. (b) Ultimate stress

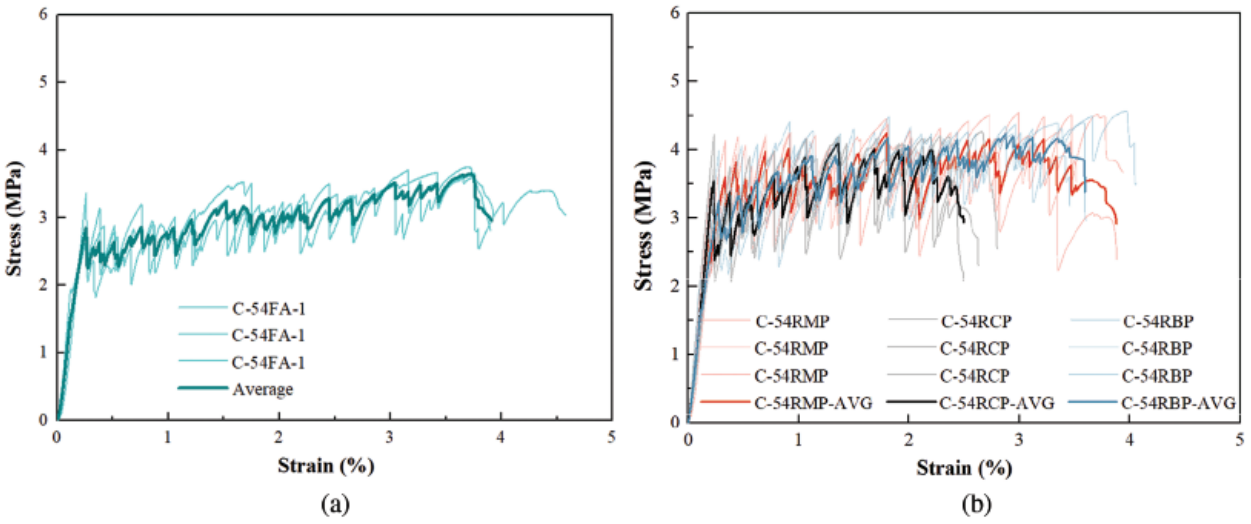

Figure 15: Comparison on the stress-strain curves of SHCC with the same content of FA and RP. (a) SHCC containing FA (Control group) and (b) SHCC containing various RPs

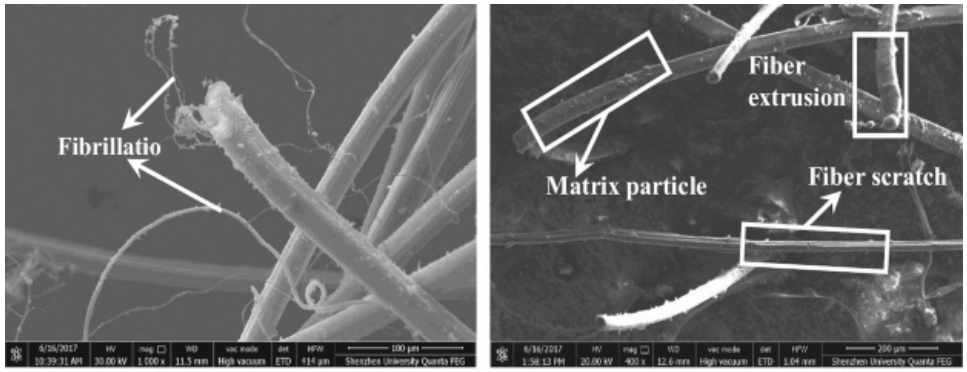

Figure 16: SEM images of fiber and fiber/matrix interface of ECC/SHCC at 28d [19]. (a) Reference cementitious composites and (b) Cementitious composites incorporating RP

3.5 Improvement in the Tensile Behavior of SHCC by Double Mixing RP and FA

This section aims to investigate the feasibility of double mixing RP and FA to achieve a more ductile SHCC; the total replacement ratios of SCM are kept at 54%, and in this case, part of RP is replaced by the same weight of FA. Fig. 17a shows the stress-strain curves of SHCC containing 54% FA, and Figs. 17b–17d shows the stress-strain curves of SHCC containing 36% RP and 18% FA. Comparing with the results shown in Figs. 17a–17d, the ultimate stress of the SHCC with the FA and RP mixture is higher than that of the SHCC with only FA; such as, the ultimate stress of C-54(RMP+FA), C-54(RCP+FA) and C-54(RBP+FA) is 7.9%, 11.4% and 14.4% higher than that of C-54FA; in addition, replacing part of the RP with FA increases the ultimate strain of RP-prepared SHCC when compared with the results shown in Figs. 11–13 and Fig. 17. Comparing with the stress-strain curves shown in Figs. 17a–17d, the ultimate strain of C-54(RMP+FA) and C-54(RBP+FA) is similar to that of C-54FA, while the ultimate strain of C-54(RCP+FA) is still lower than that of C-54FA; for instance, the ultimate strain of C-54(RMP+FA), C-54 (RCP+FA) and C-54(RBP+FA) is 3.0% lower, 30.8% lower and 3.3% higher than that of C-54FA, respectively. Combining the results shown in Figs. 11–13 shows that the double mix of RP and FA improves the strain-hardening performance of SHCC compared with the SHCC containing only RP; for instance, the ultimate strain of C-54(RMP+FA), C-54(RCP+FA) and C-54(RBP+FA) is 6.4%, 8.7% and 15.9% higher than that of C-54RMP, C-54CP and C-54RBP, respectively, as shown in Figs. 18a−18c.

The above mentioned results indicate that the double mix of RP and FA can obtain SHCC with a good ductility and strain-hardening performance. One the one hand, the addition of RP decreases the matrix strength and improves the ductility of RP prepared SHCC; in addition, the microsphere effect of FA improves the workability, and the PVA fiber can well disperse in SHCC, which helps the properties of RP-prepared SHCC. On the other hand, incorporating FA and RP further promotes the pozzolanic effect [47]; the improved micro-structure increases the frictional force between the paste and PVA fiber. In addition, the improvement in the strain-hardening of C-54(RMP+FA) and C-54(RBP+FA) is more significant than that of C-54(RCP+FA), because the activity index of RMP and RBP is high than that of RCP. Fig. 18 shows the actual cracking pattern of SHCC containing RP and the RP-FA mixture. The crack number in the SHCC with both RP and FA is higher than that of the SHCC with only RP. Therefore, double mixing RP and FA is recommended for improving the tensile behavior of SHCC; especially for SHCC with FA and RMP or RBP, the ultimate strain of the modified SHCC is similar to that of the common SHCC containing only FA, and meanwhile the ultimate stress of the modified SHCC is higher than that of the common SHCC with only FA.

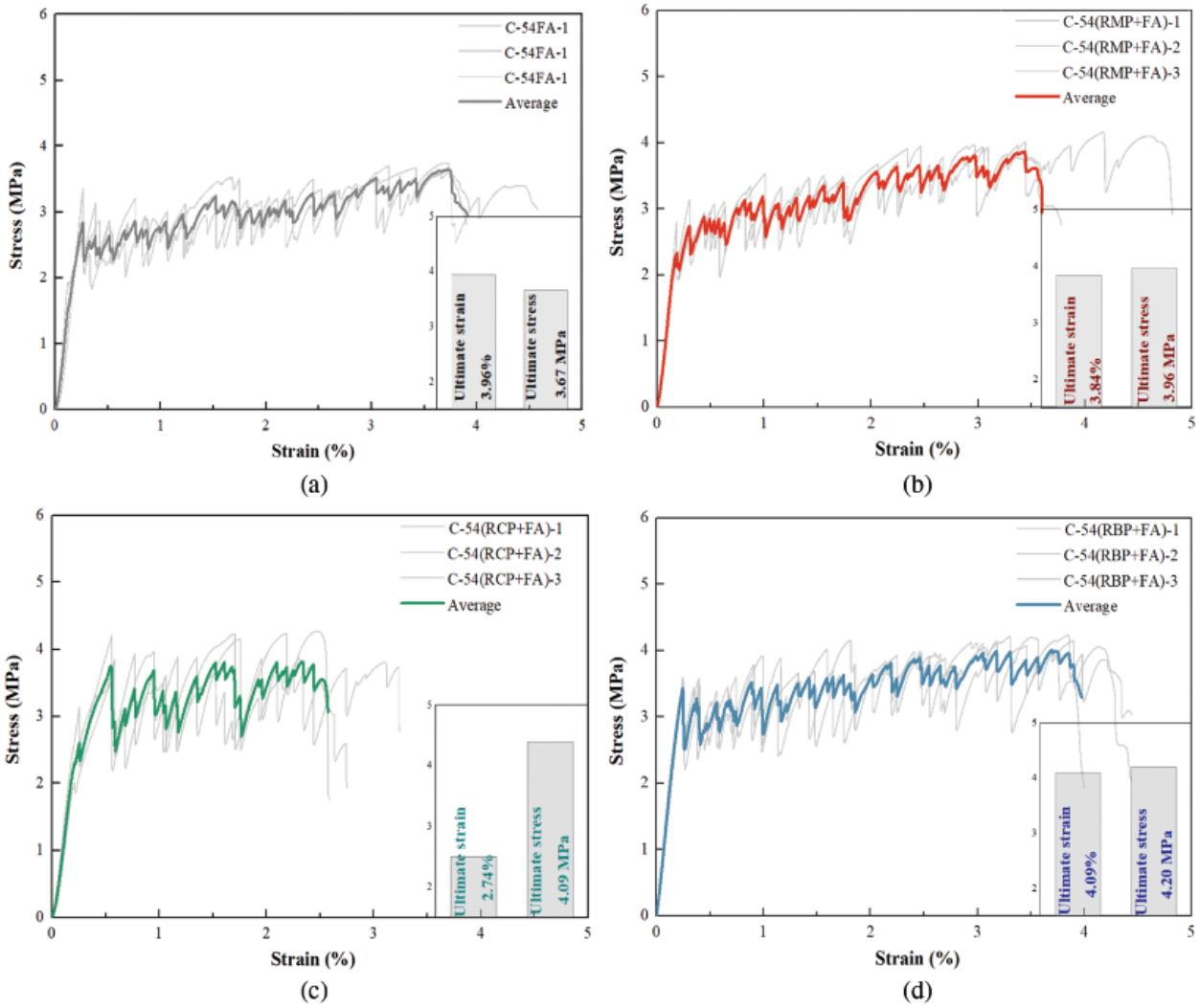

Figure 17: Stress-strain curves of SHCC containing a mixture of FA and RP when the total replacement ratios are all 54%. (a) SHCC containing FA (Control group), (b) SHCC containing a mixture of RMP and FA, (c) SHCC containing a mixture of RCP and FA and (d) SHCC containing a mixture of RBP and FA

This study investigated the micro-properties and tensile behavior of SHCC containing various types and contents of RPs, and the improvement in the strain-hardening performance by double mixing RP and FA is also investigated. However, there are some shortcomings of the current research. For example, the particle size of the RP used in this study is much lower than that of the cement and FA necessary to achieve a high reactivity, and the effects of the particle size of RP on the tensile behavior of SHCC should be investigated. In addition, the durability properties significantly impact the service life of concrete structures, and the micro-structure corresponds to the macro-properties of cement-based materials [48–55]; therefore, the durability performance and the related micro-structure of RP-prepared SHCC also needs to be studied. In addition, it is a challenge to claim that the RP are sustainable, and thus, the sustainability of RP-prepared SHCC having the same mechanical performance should be compared in a future investigation [56].

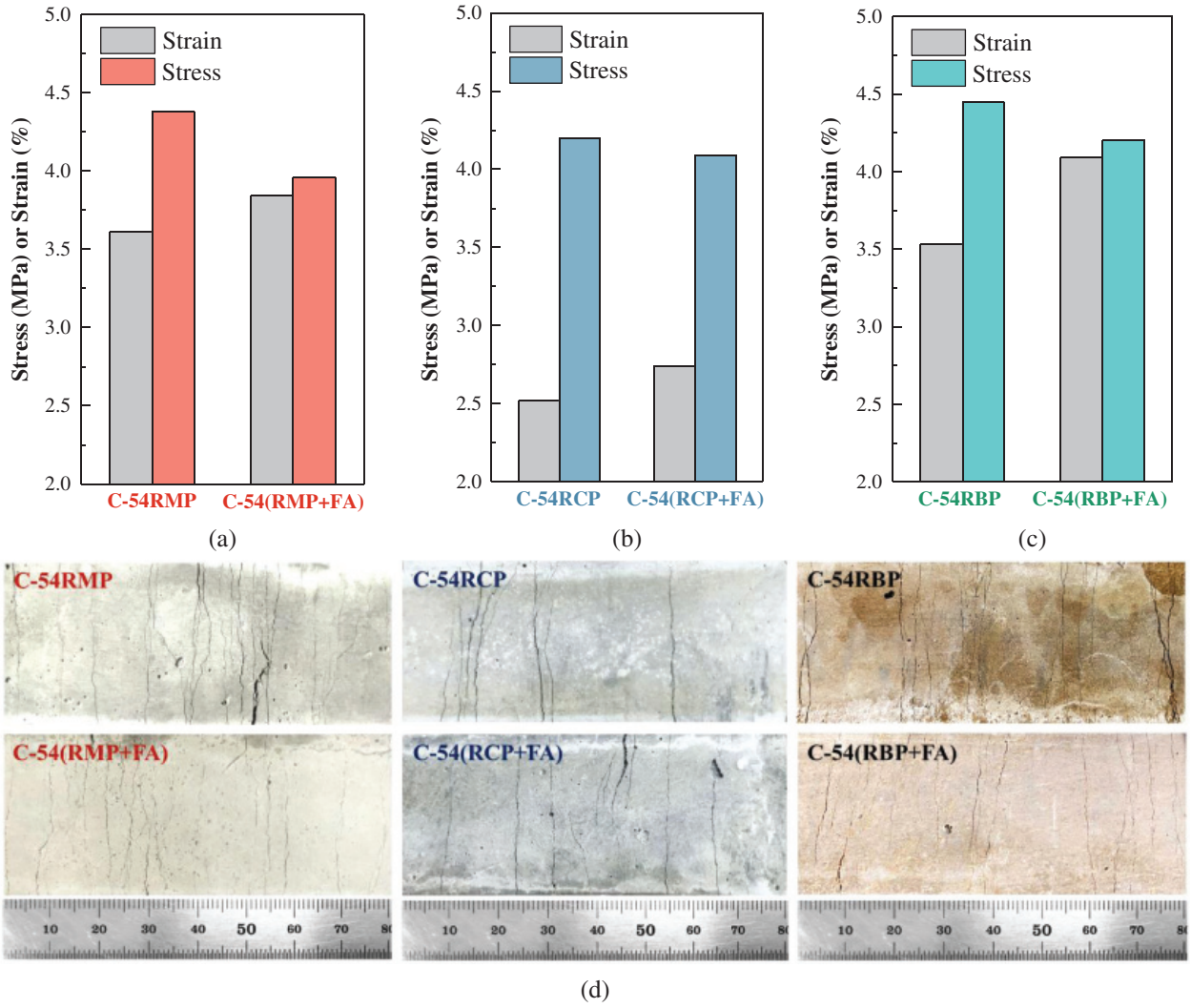

Figure 18: Comparison on the hardening behavior of SHCC containing RP and RP-FA mixture when the total replacement ratios are all 54%. (a) RMP, (b) RCP, (c) RBP and (d) Actual cracking pattern after failure

4 Conclusions

To achieve the eco-friendly and high-efficiency reclamation of construction and demolition (C&D) waste, this work investigated the micro-properties and tensile behavior of SHCC containing various types and contents of RPs from C&D waste. Based on the analysis and discussion of testing results, the following conclusions can be drawn.

1. The RP obtained from C&D waste has an irregular micro-structure. The low particle size of the RP used in this paper well fills the micro-pores of cementitious material. The high content of SiO_2 or Al_2O_3 in RMP and RBP promotes the pozzolanic effect, while RCP contains a high content of calcium carbonate; therefore, the RMP and RBP have a higher reactivity than the RCP. However, the incorporated RP decreases the hydration products content and matrix strength.
2. The activity index of FA, RMP, RCP and RBP is 83.2%, 85.5%, 78.7% and 87.0%, respectively. The incorporated RP decreases the compressive strength, and the decreased matrix strength helps the

strain-hardening performance of the SHCC; in addition, the compressive strength of the SHCC further decreases when partially replacing RP by FA.

3. Replacing cement by RP improves the ultimate strain and decreases the ultimate stress of SHCC, which means that RP incorporation improves the tensile behavior. In addition, the irregular microstructure and high reactivity of RP help the frictional force between the matrix and PVA fiber. The tensile behavior of SHCC containing RMP and RBP is better than that of SHCC containing RCP. The ultimate strain of SHCC containing 54% of FA, RMP, RBP and RCP is 3.96%, 3.61%, 2.52% and 3.53%, respectively.
4. Double mixing RP and FA can further improve the tensile behavior of SHCC, and the strain-hardening performance of SHCC with FA and RMP or RBP is close to that of SHCC with only FA. Therefore, using RP to prepare ductile SHCC is feasible, and the RMP and RBP are more appropriate in SHCC preparation than RCP.
5. The strain-stress and related parameters are used in evaluating the tensile behavior of RP prepared SHCC. However, the crack width and crack number and the micro-characteristics of cracking area were not determined in this work; thus, these properties should be determined in further study to achieve a better understand on the tensile behavior of RP-prepared SHCC.

Funding Statement: The authors gratefully acknowledge the project funded by Key R&D Program of China 2018YFD1101002 and National Natural Science Foundation of China (51778309).

Conflicts of Interest: The authors declare that they have no conflicts of interest to report regarding the present study.

References

1. Li, T., Xiao, J., Zhang, Y., Chen, B. (2019). Fracture behavior of recycled aggregate concrete under three-point bending. *Cement and Concrete Composites, 104,* 103353. DOI 10.1016/j.cemconcomp.2019.103353.
2. Liang, C. F., Ma, H. W., Pan, Y. Q., Ma, Z. M., Duan, Z. H. et al. (2019). Chloride permeability and the caused steel corrosion in the concrete with carbonated recycled aggregate. *Construction and Building Materials, 218,* 506–518. DOI 10.1016/j.conbuildmat.2019.05.136.
3. Yue, G., Ma, Z., Liu, M., Liang, C. F., Ba, G. Z. (2020). Damage behavior of the multiple ITZs in recycled aggregate concrete subjected to aggressive ion environment. *Construction and Building Materials, 245,* 118419. DOI 10.1016/j.conbuildmat.2020.118419.
4. Wu, H., Zuo, J., Zillante, G., Wang, J., Yuan, H. (2019). Construction and demolition waste research: A bibliometric analysis. *Architectural Science Review, 62(4),* 354–365. DOI 10.1080/00038628.2018.1564646.
5. Liu, T., Wang, Z., Zou, D., Zhou, A., Du, J. (2019). Strength enhancement of recycled aggregate pervious concrete using a cement paste redistribution method. *Cement and Concrete Research, 122,* 72–82. DOI 10.1016/j.cemconres.2019.05.004.
6. Xiao, J. Z., Ma, Z. M., Ding, T. (2016). Reclamation chain of waste concrete: A case study of Shanghai. *Waste Management, 48,* 334–343. DOI 10.1016/j.wasman.2015.09.018.
7. Tam, V. W., Soomro, M., Evangelista, A. C. (2018). A review of recycled aggregate in concrete applications (2000–2017). *Construction and Building Materials, 172,* 272–292. DOI 10.1016/j.conbuildmat.2018.03.240.
8. Seo, D. S., Choi, H. B. (2014). Effects of the old cement mortar attached to the recycled aggregate surface on the bond characteristics between aggregate and cement mortar. *Construction and Building Materials, 59(59),* 72–77. DOI 10.1016/j.conbuildmat.2014.02.047.
9. Wang, C., Xiao, J., Zhang, C., Xiao, X. (2020). Structural health monitoring and performance analysis of a 12-story recycled aggregate concrete structure. *Engineering Structures, 205,* 110102. DOI 10.1016/j.engstruct.2019.110102.

10. Ma, Z., Liu, M., Tang, Q., Liang, C., Duan, Z. (2020). Chloride permeability of recycled aggregate concrete under the coupling effect of freezing-thawing, elevated temperature or mechanical damage. *Construction and Building Materials, 237,* 117648. DOI 10.1016/j.conbuildmat.2019.117648.
11. Zhang, K., Xiao, J., Zhang, C. (2020). Time-dependent flexural capacity analysis of recycled aggregate concrete beams. *Engineering Structures, 218,* 110859. DOI 10.1016/j.engstruct.2020.110859.
12. Bao, J., Xue, S., Zhang, P., Dai, Z., Cui, Y. (2020). Coupled effects of sustained compressive loading and freeze–thaw cycles on water penetration into concrete. *Structural Concrete, 163(4),* 1–11. DOI 10.1002/suco.201900200.
13. Tam, V. W., Gao, X., Tam, C. M. (2005). Microstructural analysis of recycled aggregate concrete produced from two-stage mixing approach. *Cement and Concrete Research, 35(6),* 1195–1203. DOI 10.1016/j.cemconres.2004.10.025.
14. Shi, C., Li, Y., Zhang, J., Li, W., Chong, L. et al. (2016). Performance enhancement of recycled concrete aggregate–A review. *Journal of Cleaner Production, 187,* 466–472. DOI 10.1016/j.jclepro.2015.08.057.
15. Liang, C., Pan, B., Ma, Z., He, Z., Duan, Z. (2020). Utilization of CO_2 curing to enhance the properties of recycled aggregate and prepared concrete: A review. *Cement & Concrete Composites, 105,* 113446.
16. Shaikh, F. U., Chavda, V., Minhaj, N., Arel, H. S. (2018). Effect of mixing methods of nano silica on properties of recycled aggregate concrete. *Structural Concrete, 19(2),* 387–399. DOI 10.1002/suco.201700091.
17. Shaban, W. M., Yang, J., Su, H., Mo, K. H., Li, L. et al. (2019). Quality improvement techniques for recycled concrete aggregate: A review. *Journal of Advanced Concrete Technology, 17(4),* 151–167. DOI 10.3151/jact.17.151.
18. Duan, Z. H., Hou, S. D., Xiao, J. Z., Singh, A. (2020). Rheological properties of mortar containing recycled powders from construction and demolition wastes. *Construction and Building Materials, 237,* 117622. DOI 10.1016/j.conbuildmat.2019.117622.
19. Yu, K. Q., Zhu, W. J., Ding, Y., Lu, Z. D., Yu, J. T. et al. (2019). Micro-structural and mechanical properties of ultra-high performance engineered cementitious composites (UHP-ECC) incorporation of recycled fine powder (RFP). *Cement and Concrete Research, 124,* 105813. DOI 10.1016/j.cemconres.2019.105813.
20. Duan, Z. H., Hou, S. D., Xiao, J. Z., Li, B. (2020). Study on the essential properties of recycled powders from construction and demolition waste. *Journal of Cleaner Production, 253,* 119865. DOI 10.1016/j.jclepro.2019.119865.
21. Ma, Z.M., Tang, Q., Wu, H. X., Xu, J. G., Liang, C. F. (2020). Mechanical properties and water absorption of cement composites with various fineness and contents of waste brick powder from C&D waste, Cement and Concrete Composites, *114,* 103758. DOI 10.1016/j.cemconcomp.2020.103758.
22. Tang, Q., Ma, Z. M., Wu, H. X., Wang, W. (2020). The utilization of eco-friendly recycled powder from concrete and brick waste in new concrete: A critical review. *Cement and Concrete Composites, 2020,* 103807.
23. Mehdizadeh, H., Ling, T. C., Cheng, X., Mo, K. H. (2020) Effect of particle size and CO_2 treatment of waste cement powder on properties of cement paste. *Canadian Journal of Civil Engineering, 0574,* 1–37. DOI 10.1139/cjce-2019-0574.
24. Singh, A., Arora, S., Sharma, V., Bhardwaj, B. (2019). Workability retention and strength development of self-compacting recycled aggregate concrete using ultrafine recycled powders and silica fume. *Journal of Hazardous, Toxic, and Radioactive Waste, 23(4),* 04019016. DOI 10.1061/(ASCE)HZ.2153-5515.0000456.
25. Liu, Q., Li, B., Xiao, J., Singh, A. (2020). Utilization potential of aerated concrete block powder and clay brick powder from C&D waste. *Construction and Building Materials, 238,* 117721. DOI 10.1016/j.conbuildmat.2019.117721.
26. Xiao, J., Ma, Z., Sui, T., Akbarnezhad, A., Duan, Z. (2018). Mechanical properties of concrete mixed with recycled powder produced from construction and demolition waste. *Journal of Cleaner Production, 188,* 720–731. DOI 10.1016/j.jclepro.2018.03.277.
27. Ortega, J. M., Letelier, V., Solas, C., Moriconi, G., Climent, M. A., Sanchez, I. (2018). Long-term effects of waste brick powder addition in the microstructure and service properties of mortars. *Construction and Building Materials, 182,* 691–702. DOI 10.1016/j.conbuildmat.2018.06.161.

28. Ma, Z., Liu, M., Duan, Z., Liang, C., Wu, H. (2020). Effects of active waste powder obtained from C&D waste on the microproperties and water permeability of concrete. *Journal of Cleaner Production, 257,* 120518. DOI 10.1016/j.jclepro.2020.120518.
29. Son, M., Kim, G., Kim, H., Lee, S., Nam, J. et al. (2020). Effects of the strain rate and fiber blending ratio on the tensile behavior of hooked steel fiber and polyvinyl alcohol fiber hybrid reinforced cementitious composites. *Cement and Concrete Composites, 106,* 103482. DOI 10.1016/j.cemconcomp.2019.103482.
30. Son, M., Kim, G., Kim, H., Lee, S., Kobayashi, K. (2019). Effects of the strain rate and fiber blending ratio on the tensile behavior of hooked steel fiber and polyvinyl alcohol fiber hybrid reinforced cementitious composites. *Cement and Concrete Composites, 106,* 103482. DOI 10.1016/j.cemconcomp.2019.103482.
31. Zhang, P., Dai, Y. Q., Wang, W. T., Yang, J. B., Mo, L. W. et al. (2020). Effects of magnesium oxide expansive agents on the self-healing performance of microcracks in Strain-Hardening Cement-based Composites (SHCC). *Materials Today Communications, 2020,* 101421.
32. Yu, J., Jiang, F., Yu, K., Dong, F., Duan, X. (2020). Deformability enhancement of fiber-reinforced cementitious composite by incorporating recycled powder. *Journal of Reinforced Plastics and Composites, 39(3–4),* 119–131. DOI 10.1177/0731684419877251.
33. Wang, W., Wu, H., Ma, Z., Wu, R. (2020). Using eco-friendly recycled powder from CDW to prepare strain hardening cementitious composites (SHCC) and properties determination. *Materials, 13(5),* 1143. DOI 10.3390/ma13051143.
34. Yang, D., Liu, M., Ma, Z. (2020). Properties of the foam concrete containing waste brick powder derived from construction and demolition waste. *Journal of Building Engineering, 32,* 101509. DOI 10.1016/j.jobe.2020.101509.
35. Zijl, G. P. A. G. V., Wittmann, F. H., Oh, B. H., Kabele, P., Filho, R. D. T. et al. (2012). Durability of strain-hardening cement-based composites (SHCC). *Materials and Structures, 45(10),* 1447–1463. DOI 10.1617/s11527-012-9845-y.
36. Zijl, G. P. A. G. V., Slowik, V., Filho, R. D. T., Wittmann, F. H., Mihashi, H. (2015). Comparative testing of crack formation in strain-hardening cement-based composites (SHCC). *Materials and Structures, 49(4),* 1175–1189. DOI 10.1617/s11527-015-0567-9.
37. Zhang, P., Dai, Y., Ding, X., Zhou, C., Zhao, T. (2018). Self-healing behaviour of multiple microcracks of strain hardening cementitious composites (SHCC). *Construction and Building Materials, 169,* 705–715. DOI 10.1016/j.conbuildmat.2018.03.032.
38. Zhang, P., Wang, P., Hou, D., Liu, Z., Haist, M. et al. (2017). Application of neutron radiography in observing and quantifying the time-dependent moisture distributions in multi-cracked cement-based composites. *Cement and Concrete Composites, 78,* 13–20. DOI 10.1016/j.cemconcomp.2016.12.006.
39. Xue, S. B., Zhang, P., Bao, J. W., He, L. F., Hu, Y. et al. (2020). Comparison of mercury intrusion porosimetry and multi-scale X-ray CT on characterizing the microstructure of heat-treated cement mortar. *Materials Characterization, 160,* 110085. DOI 10.1016/j.matchar.2019.110085.
40. Lorenzoni, R., Curosu, I., Leonard, Fabién, Paciornik, S., Bruno, G. (2020). Combined mechanical and 3D-microstructural analysis of strain-hardening cement-based composites (SHCC) by *in-situ* X-ray microtomography. *Cement and Concrete Research, 136,* 106139. DOI 10.1016/j.cemconres.2020.106139.
41. Zhao, K. Y., Qiao, Y., Zhang, P., Bao, J. W., Tian, Y. P. (2020). Experimental and numerical study on chloride transport in cement mortar during drying process. *Construction and Building Materials, 258,* 119655. DOI 10.1016/j.conbuildmat.2020.119655.
42. Qian, D., Yu, R., Shui, Z., Sun, Y., He, Y. (2020). A novel development of green ultra-high performance concrete (UHPC) based on appropriate application of recycled cementitious material. *Journal of Cleaner Production, 261,* 121231. DOI 10.1016/j.jclepro.2020.121231.
43. Shao, J., Gao, J., Zhao, Y., Chen, X. (2019). Study on the pozzolanic reaction of clay brick powder in blended cement pastes. *Construction and Building Materials, 213,* 209–215. DOI 10.1016/j.conbuildmat.2019.03.307.
44. Yu. J. T., Tian, L. K., Wang, Y. C. (2019). Mechanical property of recycled micro-powder cementitious composites with ultra-high ductility. *Materials Reports, 33,* 1328–1334. DOI 10.11896/cldb.17110286.

45. Cao, M., Xu, L., Zhang, C. (2015). Review on micromechanical design, performance and development tendency of engineered cementitious composite. *Journal of the Chinese Ceramic Society, 43(5),* 632–642.
46. Liu, C. L., Bi, Y. Z., Hua, Y. (2017). Mechanical properties of PVA-ECC with high volume fly ash and mechanism analysis of fly ash. *Bulletin of the Chinese Ceramic Society. 11,* 3739–3744. DOI 10.16552/j.cnki.issn1001-1625.2017.11.027.
47. Cheng, Y. H., Huang, F., Liu, R., Hou, J. L., Li, G. L. (2016). Test research on effects of waste ceramic polishing powder on the permeability resistance of concrete. *Materials and Structures, 49(3),* 729–738. DOI 10.1617/s11527-015-0533-6.
48. Bao, J. W., Xue, S. B., Zhang, P., Dai, Z. Z., Cui, Y. F. (2020). Coupled effects of sustained compressive loading and freeze–thaw cycles on water penetration into concrete. *Structural Concrete, 163(4),* 840. DOI 10.1002/suco.201900200.
49. Liu, C., Liu, H. W., Xiao, J. Z., Bai, G. L. (2020). Effect of old mortar pore structure on relative humidity response of recycled aggregate concrete. *Construction and Building Materials, 247,* 118600. DOI 10.1016/j.conbuildmat.2020.118600.
50. Ma, Z. M., Tang, Q., Yang, D. Y., Ba, G. Z. (2019). Durability studies on the recycled aggregate concrete in china over the past decade: A review. *Advances in Civil Engineering, 2019(2),* 1–19. DOI 10.1155/2019/4073130.
51. Wang, W. T., Zhao, K. Y., Zhang, P., Bao, J. W., Xue, S. B. (2020). Application of three self-developed ECT sensors for monitoring the moisture content in sand and mortar. *Construction and Building Materials, 10,* 121008. DOI 10.1016/j.conbuildmat.2020.121008.
52. Xue, S. B., Meng, F. Q., Zhang, P., Bao, J. W. Wang, J. J. et al. (2020). Influence of water re-curing on microstructure of heat-damaged cement mortar characterized by low-field NMR and MIP. *Construction and Building Materials, 262,* 120532.
53. Xiao, J. Z., Li, Z. W., Xie, Q. H., Shen, L. M. (2016). Effect of strain rate on compressive behaviour of high-strength concrete after exposure to elevated temperatures. *Fire Safety Journal, 83,* 25–37. DOI 10.1016/j.firesaf.2016.04.006.
54. Bao, J. W., Zhang, P., Li, S. G., Xue, S. B., Cui, Y. F. et al. (2020). Influence of exposure environments and moisture content on water repellency of surface impregnation of cement-based materials. *Journal of Materials Research and Technology, 9(6),* 12115–12125. DOI 10.1016/j.jmrt.2020.08.046.
55. Xiao, J. Z., Holger, S., Cindy, D. E., Gert, K. (2004). Wedge splitting test on fracture behaviour of ultra high strength concrete. *Construction and Building Materials, 18(6),* 359–365. DOI 10.1016/j.conbuildmat.2004.04.016.
56. Visintin, P., Xie, T., Bennett, B. (2020). A large-scale life-cycle assessment of recycled aggregate concrete: The influence of functional unit, emissions allocation and carbon dioxide uptake. *Journal of Cleaner Production, 248,* 119243. DOI 10.1016/j.jclepro.2019.119243.